Inorg. Chem. **2003**, *42*, 8646–8651

Structural Analysis of Nine-Coordinate Lanthanide Complexes: Steric Control of the Metal–Water Distance Across the Series

David Parker,* Horst Puschmann, Andrei S. Batsanov, and Kanthi Senanayake

Department of Chemistry, University of Durham, South Road, Durham DH1 3LE, U.K.

Received June 20, 2003

The structures of 10 isomorphous lanthanide (Ln) complexes of a chiral DOTA tetra-amide ligand (L^1), $[LnL^1(H_2O)](CF_3SO_3)_3 \cdot 3H_2O$, crystallizing in space group $P2_1$, have been studied by single-crystal X-ray diffraction. The Ln coordination is a O_4N_4 square antiprism, the O_4 base of which is capped by an aqua ligand. The sterically demanding position of the latter results in the lengthening of the Ln–OH_2 distance along the Pr to Lu series by 0.06 Å (after allowing for the lanthanide contraction). In parallel, the distance between the bound water oxygen and the second-sphere water oxygen is reduced from 3.17 Å (Pr) to 3.04 Å (Lu), consistent with the enhanced hydrogen bond acceptor ability of the coordinated water oxygen across the series. A Cambridge Structural Database survey of $[Ln(H_2O)_9](CF_3SO_3)_3$ salts (space group $P6_3/m$) and of six reported isostructural complexes of DOTA [L^2] revealed a similar trend. The implications of the resultant destabilization of the ground state structure for the water interchange process are discussed.

Introduction

An understanding of the factors determining the rate of dissociative water exchange at a metal center requires an appreciation of features that control not only the relative stability and position of the transition state structure but also the energy of the ground state structure.[1,2] Given that, for a dissociative water interchange process with an early transition state, a lengthening of the metal−water bond distance (destabilization of the ground state) will be linked to a faster rate of water exchange, it is then important to evaluate critically the factors that control the metal−water distance, in the ground state structure. This can be assessed most directly by a comparison of X-ray structural data, defining the metal water oxygen distance, for structurally related series of complexes,[3a] crystallizing in a common space group.

The need to improve our understanding of water exchange mechanisms has been driven over the past few years by the relationship to the development of improved MRI contrast agents.[4] Complexes of gadolinium, e.g., $[GdDTPA(H_2O)]^{2-}$ and $[GdDOTA(H_2O)]^-$ (DOTA = L^2 = 1,4,7,10-tetraazacyclododecanetetraacetate), are used routinely in thousands of MRI scans each year, and they function by catalyzing the rate of relaxation of the water protons. The efficiency of this process can be limited by the rate of water interchange at the paramagnetic center, so that a great deal of research has been directed toward improving our understanding of the determinants of this process.[5,6] Important features defined recently for nine-coordinate systems include the coordination geometry at the gadolinium center[7] (e.g., regular vs twisted square antiprismatic), and the nature of the second sphere of hydration,[3,8] in turn, defined by ligand hydrophobicity[9] and the nature of the counterions.[10] The former factor has

* To whom correspondence should be addressed. E-mail: david.parker@durham.ac.uk.

(1) Eigen, M. *Pure Appl. Chem.* **1963**, *6*, 105. Wilkins, R. G.; Eigen, M. *Adv. Chem. Ser.* **1965**, *49*, 55. Swaddle, T. W. *Comments Inorg. Chem.* **1991**, *12*, 237.
(2) Richens, D. T. *The Chemistry of Aqua Ions*; Wiley: New York, 1997.
(3) (a) Dickins, R. S.; Parker, D.; Puschmann, H.; Crossland, C.; Howard, J. A. K. *Chem. Rev.* **2002**, *102*, 1977−2010. (b) Beeby, A.; Clarkson, I. M.; Dickins, R. S.; Faulkner, S.; Parker, D.; Royle, L.; de Sousa, A. S.; Williams, J. A. G.; Woods, M. *J. Chem. Soc., Perkin Trans. 2* **1999**, 493.
(4) *The Chemistry of Contrast Agents in Medical Magnetic Resonance Imaging*; Merbach, A. E., Toth, K. Eds.; Wiley: New York, 2001.
(5) Caravan, P.; Ellison, J. J.; McMurry, T. J.; Lauffer, R. B. *Chem. Rev.* **1999**, *99*, 2293.
(6) Aime, S.; Botta, M.; Fasano, M.; Terreno, E. *Chem. Soc. Rev.* **1998**, *27*, 19.
(7) Aime, S.; Barge, A.; Botta, M.; de Sousa, A. S.; Parker, D. *Angew. Chem., Int. Ed.* **1998**, *37*, 2673−2675. Woods, M.; Aime, S.; Botta, M.; Howard, J. A. K.; Moloney, J. M.; Navet, M.; Port, M.; Rousseaux, O. *J. Am. Chem. Soc.* **2000**, *122*, 9781. Dunand, F. A.; Aime, S.; Merbach, A. E. *J. Am. Chem. Soc.* **2000**, *122*, 1506.
(8) Botta, M., *Eur. J. Inorg. Chem.*, **2000**, 399.
(9) Aime, S.; Barge, A.; Batsanov, A. S.; Botta, M.; Delli Castelli, D.; Fedeli, F.; Mortillaro, A.; Parker, D.; Puschmann, H. *Chem. Commun.* **2002**, 1120.
(10) Barge, A.; Botta, M.; Parker, D.; Puschmann, H. *Chem. Commun.* **2003**, 1386.

10.1021/ic030203z CCC: $25.00
Published on Web 12/02/2003

also been linked to the longer Ln−OH_2 bond distances generally observed in twisted square-antiprismatic coordination environments.[3b,11]

Here, we seek to assess the structural features of three lanthanide complex systems, each of which is nine-coordinate, and can be regarded as adopting a monocapped square-antiprismatic coordination geometry. The first series is the aqua ion complexes, $[Ln(OH_2)_9]^{3+}$, which crystallize as their triflate salts in the common space group $P6_3/m$. Although each complex formally adopts a tricapped trigonal prismatic structure, this can also be viewed as a monocapped square antiprism (Figure 1). Information on a short series of isomorphous and isostructural $[LnDOTA(H_2O)]^-\cdot 4H_2O$ complexes (Ln = Pr, Nd, Eu, Gd, Ho, Lu) has also been reported recently, allowing a comparative assessment.[12] Finally, data are reported and analyzed for the series of cationic complexes based on the chiral tetra-amide ligand, (*RRRR*) or (*SSSS*) in the case of Sm and Eu. This ligand forms trihydrated monoaqua complexes, $[LnL^1(H_2O)](CF_3SO_3)_3\cdot 3H_2O$, in a square-antiprismatic geometry across the whole of the lanthanide series.[9,13] Results are presented for nine lanthanide complexes, crystallizing in a common space group, and the data compared to those obtained for the aqua ion and $[LnDOTA(H_2O)]^-$ complexes.

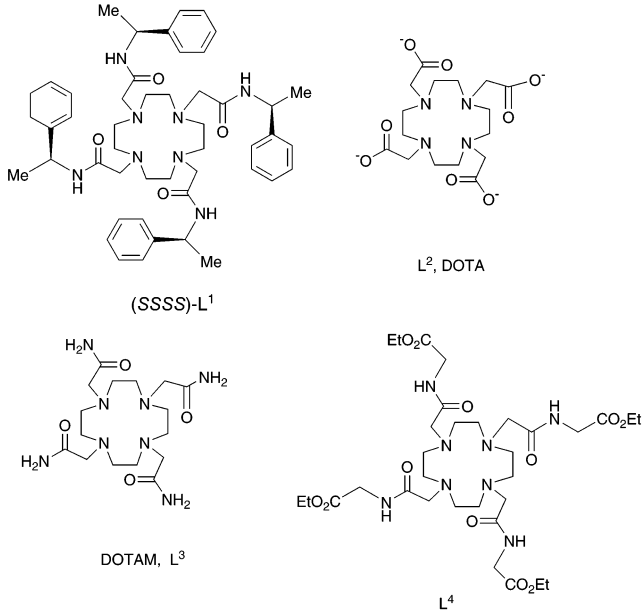

Experimental Section

X-ray diffraction experiments (see Table 1) for Nd and Gd were carried out on a SMART 3-circle diffractometer with an APEX CCD area detector, using graphite-monochromated Mo Kα radiation

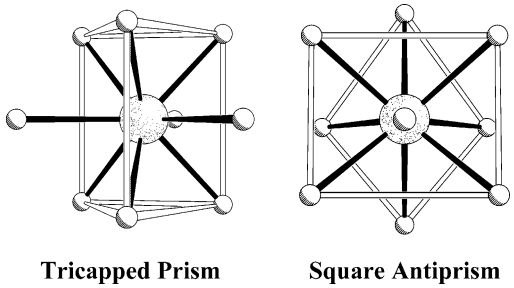

Figure 1. Views of the crystal structure of $[La(H_2O)_9](CF_3SO_3)_3$, showing the relationship between the tricapped trigonal prismatic structure and a monocapped square-antiprismatic coordination environment. These diagrams both depict the exact same structure. The "hollow" lines have no chemical significance.

($\bar{\lambda}$ = 0.71073 Å) from a 60 W Mo target microfocus Bede Microsource X-ray generator with glass polycapillary X-ray optics. Other experiments were were carried out on SMART 3-circle diffractometer with a 6K CCD area detector, using sealed-tube graphite-monochromated Mo Kα radiation. The low temperature (120 K) of the crystals was maintained with a Cryostream open-flow N_2 cryostat (Oxford Cryosystems). A full sphere of reciprocal space was covered by 4−6 sets of narrow (0.3°) ω scans, each set with different ω and/or 2θ angles. The intensities were corrected for absorption by a semiempirical method based on Laue equivalents[20] (for Eu by numerical integration based on real crystal shape). The structures were solved by analogy with isomorphous complexes, and all were refined by full-matrix least-squares against F^2 of all data, using SHELXTL software.[21] The absolute structures for all compounds were confirmed from anomalous dispersion, using the Flack method.[22] The triflate ligand disorder was modeled by two orientations, differing by a libration around the S(2) atom, but large displacement parameters and high (>1 eÅ^{-3}) diffuse electron density indicate more complex disorder. Full crystallographic data, excluding structure factors, are provided in Electronic Supplementary Information and have been deposited at the Cambridge Crystallographic Data Centre, CCDC-213665 to 213670.

Each of these complexes, as well as the previously reported Yb, Tb, and Er[9,13] ones, form isomorphous monoclinic crystals (space group $P2_1$), the asymmetric unit of which comprises one cation, three triflate anions (one of them disordered to a varying degree), and three water molecules of crystallization, linked by a 3-dimensional network of hydrogen bonds. It is noteworthy that crystal-

(11) Kang, S. I.; Ranganathan, R. S.; Emswiler, J. E.; Kumar, K.; Gougoutas, J. Z.; Malley, M. F.; Tweedle, M. F. *Inorg. Chem.* **1993**, *32*, 2912.
(12) Benetello, F.; Bombieri, G.; Calabi, L.; Aime, S.; Botta, M. *Inorg. Chem.* **2003**, *42*, 148−157. Spirlet, M. R.; Rebizant, J.; Desreux, J. F.; Loncin, M. F. *Inorg. Chem.* **1984**, *23*, 359−363. Chang, C. A.; Francesconi, L. C.; Malley, M. F.; Kumar, K.; Gougoutas, J. Z.; Tweedle, M. F.; Lee, D. W.; Wilson, C. F. *Inorg. Chem.* **1993**, *32*, 3501−3508.
(13) Dickins, R. S.; Howard, J. A. K.; Maupin, C. L.; Moloney, J. M.; Parker, D.; Riehl, J. P.; Siligardi, G.; Peacock, R. D. *Chem. Eur. J.* **1999**, *5*, 1095. Batsanov, A. S.; Beeby, A.; Bruce, J. I.; Howard, J. A. K.; Kenwright, A. M.; Parker, D. *Chem. Commun.* **1999**, 1011.
(14) Shannon, R. D. *Acta Crystallogr.* **1976**, *32*, 751.
(15) Crystals grown from aqueous ethanol sometimes included a small amount of ethanol and crystallized in *I*2, with two independent molecules in the unit cell. More extensive disorder was found in the lattice, and the Ln−OH_2 bond distances were 0.06 and 0.05 Å shorter than those for complexes in $P2_1$ containing only water (Er and Gd or Pr, respectively), with a different pattern of hydrogen bonding between the bound water and solvent and between anions and the solvent.[9]
(16) For related, but less well exemplified, analyses of lanthanide−ligand bond variations across the series, involving tetraazaphisphinates and texaphyrins, respectively, see ref 12 (Bombieri et al.) and the following: Aime, S.; Batsanov, A. S.; Botta, M.; Dickins, R. S.; Faulkner, S.; Foster, C. E.; Harrison, A.; Howard, J. A. K.; Moloney, J. M.; Norman, T. J.; Parker, D.; Royle, L.; Williams, J. A. G. *J. Chem. Soc., Dalton Trans.* **1997**, 3623. Lisowski, J.; Sessler, J. L.; Lynch, V.; Mody, T. D. *J. Am. Chem. Soc.* **1995**, *117*, 2273.
(17) Dunand, F. A.; Dickins, R. S.; Merbach, A. E.; Parker, D. *Chem. Eur. J.* **2001**, *7*, 5160. Pubanz, D.; Gonzalez, G.; Powell, D. H.; Merbach, A. E. *Inorg. Chem.* **1995**, *34*, 4447.
(18) Zhang, S.; Wu, K.; Sherry, A. D. *J. Am. Chem. Soc.* **2002**, *124*, 4226.
(19) de Bari, L.; Dickins, R. S.; Parker, D.; Pintacuda, G.; Salvadori, P. *J. Am. Chem. Soc.* **2000**, *122*, 9257.
(20) *SADABS*, version 2.03; Bruker AXS: Madison, WI, 2001.
(21) *SHELXTL*, version 5.1; Bruker AXS: Madison, WI, 1997.
(22) Flack, H. D. *Acta Crystallogr., Sect. A* **1983**, *39*, 870.

Table 1. Crystal Data for $[C_{48}H_{66}N_8O_5Ln]^{3+}(CF_3SO_3^-)_3 \cdot 3H_2O$[a]

compd	Pr	Nd	Sm	Eu	Gd	Tb[b]	Dy	Er[b]	Yb[b]	Lu[b]
configuration	*RRRR*	*RRRR*	*SSSS*	*SSSS*	*RRRR*	*RRRR*	*RRRR*	*RRRR*	*RRRR*	*RRRR*
fw	1477.26	1480.59	1486.70	1488.31	1493.60	1495.27	1498.85	1503.61	1509.39	1511.32
a, Å	14.761(3)	14.757(3)	14.685(4)	14.674(3)	14.666(3)	14.613(3)	14.532(2)	14.473(1)	14.390(1)	14.387(2)
b, Å	11.596(2)	11.587(3)	11.658(3)	11.668(3)	11.674(2)	11.728(2)	11.805(2)	11.845(1)	11.928(1)	11.931(1)
c, Å	19.348(3)	19.305(5)	19.302(6)	19.276(3)	19.236(4)	19.241(4)	19.247(3)	19.217(2)	19.300(1)	19.289(2)
β, deg	101.58(1)	101.55(1)	101.78(1)	101.77(2)	101.78(1)	101.94(1).	102.16(1)	102.4(1)	102.7(1)	102.7(1)
V, Å^3	3245.4(10)	3234.1(14)	3234.9(16)	3230.8(12)	3224.0(11)	3226.2(11)	3227.7(9)	3218.2(5)	3232.1(4)	3230.1(5)
μ, mm^{-1}	0.94	1.00	1.00	1.16	1.22	1.29	1.35	1.50	1.64	1.72
reflns collected	60915	56440	33678	58652	48792	36411	59411	53154	40617	47962
unique reflns	18934	18146	13969	18861	18404	14049	18798	23033	17088	15564
R_{int}	0.062	0.017	0.107	0.012	0.025	0.052	0.038	0.0207	0.0250	0.0824
reflns $I > 2\sigma(I)$	17822	17655	8420	17941	17488	14049	17245	21765	16442	15040
R [$I > 2\sigma(I)$]	0.030	0.025	0.056	0.027	0.028	0.032	0.030	0.0256	0.021	0.029
R_w (F^2), all data	0.073	0.065	0.077	0.066	0.067	0.078	0.075	0.0638	0.051	0.057

[a] $T = 120$ K, monoclinic, space group $P2_1$ (No. 4), $Z = 2$. [b] Previously published.[9,13]

Table 2. Bond Distances (Å) and Torsion Angles (deg) in for $[C_{48}H_{66}N_8O_5Ln]^{3+}(CF_3SO_3^-)_3 \cdot 3H_2O$

	Pr	Nd	Sm	Eu	Gd	Tb[a]	Dy	Er[a]	Yb[a]	Lu[a]
Ln−O(1)	2.428(2)	2.414(2)	2.374(4)	2.377(2)	2.368(2)	2.355(2)	2.344(2)	2.321(1)	2.274(2)	2.292(2)
Ln−O(2)	2.403(2)	2.392(2)	2.352(4)	2.355(2)	2.346(2)	2.350(2)	2.315(2)	2.296(2)	2.274(2)	2.273(2)
Ln−O(3)	2.434(2)	2.419(2)	2.383(4)	2.379(2)	2.367(2)	2.333(2)	2.336(2)	2.310(1)	2.288(2)	2.283(2)
Ln−O(4)	2.415(2)	2.402(2)	2.362(4)	2.361(2)	2.353(2)	2.331(2)	2.317(2)	2.294(1)	2.298(2)	2.273(2)
Ln−O(5)	2.516(3)	2.501(2)	2.495(4)	2.482(2)	2.460(2)	2.461(3)	2.454(2)	2.432(2)	2.440(2)	2.426(2)
Ln−N(1)	2.696(2)	2.677(2)	2.647(5)	2.643(2)	2.633(2)	2.624(3)	2.620(2)	2.605(2)	2.598(2)	2.592(2)
Ln−N(2)	2.738(2)	2.715 (2)	2.685(5)	2.680(2)	2.670(2)	2.642(3)	2.654(2)	2.639(2)	2.636(2)	2.636(2)
Ln−N(3)	2.708(2)	2.690(2)	2.654(5)	2.655(2)	2.650(2)	2.664(3)	2.644(2)	2.629(2)	2.626(2)	2.623(2)
Ln−N(4)	2.746(2)	2.725(2)	2.697(5)	2.689(2)	2.675(2)	2.669(3)	2.658(2)	2.636(2)	2.630(3)	2.623(3)
N(1)C(10)C(11)O(1)	−36.2(4)	−36.3(3)	35.5(10)	35.1(3)	−35.0(4)	−33.2(5)	−34.3(3)	−34.4(3)	−33.9(3)	−33.7(3)
N(2)C(20)C(21)O(2)	−22.8(3)	−23.4(3)	19.3(9)	23.9(3)	−25.1(4)	−24.6(5)	−25.7(4)	−26.5(3)	−26.3(3)	−26.3(5)
N(3)C(30)C(31)O(3)	−32.7(3)	−31.8(3)	33.4(8)	32.1(3)	−31.4(3)	−30.7(5)	−29.8(4)	−29.3(3)	−28.8(3)	−28.5(4)
N(4)C(40)C(41)O(4)	−31.5(3)	−31.5(3)	32.7(7)	30.9(3)	−30.5(3)	−30.0(5)	−28.9(3)	−28.4(3)	−26.9(3)	−27.4(4)
N(1)C(1)C(2)N(2)	58.0(3)	57.4(2)	−54.8(7)	−57.1(3)	57.0(3)	56.7 (4)	57.3(3)	57.0(2)	56.8(3)	56.7(3)
N(2)C(3)C(4)N(3)	61.6(3)	61.1(2)	−59.6(7)	−60.5(3)	60.5(3)	60.5(4)	60.1(3)	59.8(2)	59.5(3)	59.7(3)
N(3)C(5)C(6)N(4)	58.3(3)	58.0(2)	−56.1(7)	−57.4(3)	56.9(3)	56.9(4)	57.4(3)	56.9(2)	56.4(3)	56.8(3)
N(4)C(7)C(8)N(1)	61.1(3)	60.5(2)	−58.7(7)	−60.2(3)	59.5(3)	59.2(4)	59.5(3)	59.3(2)	59.3(3)	59.2(3)

[a] Previously published.[9,13]

lization from water−methanol solutions gives initially the much less stable crystals of the space group *I*2 (also comprising an isomorphous series),[9] which convert into the $P2_1$-type if left in the mother liquor; in some cases, both forms were crystallizing simultaneously.

Results

CSD Database Analysis. Analysis of the Cambridge Crystallographic Database reveals that there are 44 nona-aqua complexes reported with a triflate counterion; for those complexes that crystallize in the space group $P6_3/m$, there are two M−OH_2 distances. One of these characterizes the distance between the Ln ion and the six vertices of a trigonal prism, and the other represents the longer Ln−OH_2 distance of the three capping water molecules. The variation of the Ln−OH_2 distance faithfully follows the ionic radius change across the series for the shorter bonds to the vertices of the prism. Thus, when these distances are normalized, to account for the ionic radius change[14] (Figure 2), the Ln−OH_2 distance is clearly seen to be invariant across the series. However, for the longer bond to each "capping" position, the distance lengthens across the series and is about 0.06 Å longer for Lu than Ce. Presumably, this variation reflects the ease of packing the nine water molecules about the spherical ion, with the three longer bonds resulting from a minimization of steric repulsion between adjacent water molecules.

Consideration of the six reported complexes of $[LuDOTA(H_2O)]^- \cdot 4H_2O$ that crystallize in *P*1 (Ln = Pr, Nd, Eu, Gd, Ho, Lu) in a monocapped square-antiprismatic coordination geometry (SAP; twist angle of the N_4/O_4 planes is typically 39°) reveals a similar trend. In this case, the normalized Ln to ligand oxygen distances also faithfully follow the ionic radius variation (Table 2), whereas the Ln−OH_2 distances are longer for the smaller ions and increase regularly by 0.04 Å from Pr to Lu (Figure 3). Thus, the lanthanide contraction is accommodated by changes in the bond distances to the ligand donors (the Ln−N variation follows the same trend),

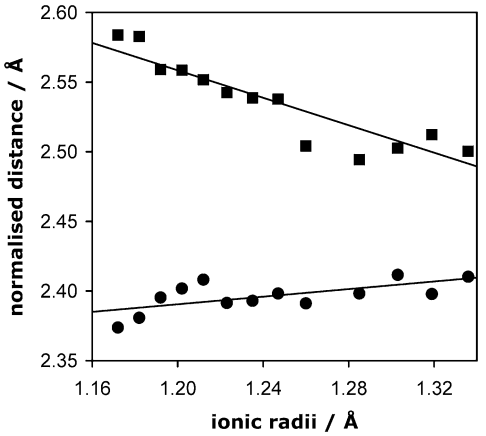

Figure 2. Variation of the Ln−OH_2 distances in X-ray structures of $[Ln(OH_2)_9](CF_3SO_3)_3$ reported in the CSD that adopt a $P6_3/m$ space group. Distances have been normalized (Gd as reference point) to account for the ionic radius variation. The longer bonds (■) represent the lanthanide−water bond length to each of the three water molecules capping the faces of the trigonal prism.

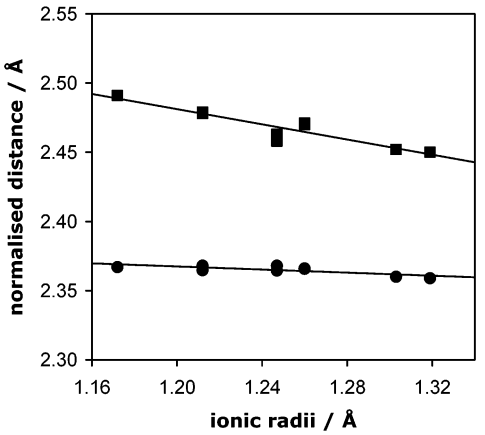

Figure 3. Variation of the Ln−OH_2 distances (upper: ■) and the lanthanide−ligand oxygen distances for the isomorphous series [LnDOTA-(OH_2)]$^-$·4H_2O (Ln = Pr, Nd, Eu, Gd, Ho, Lu) crystallizing in *P*1. Lanthanide oxygen distances have been normalized (to Gd), to account for the ionic radius variation.

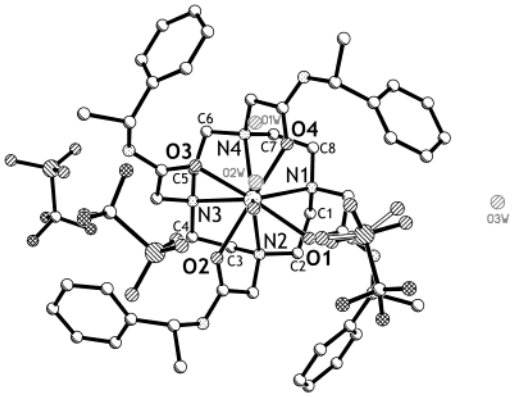

Figure 4. Views of the structure of [$TbL^1(OH_2)$]$(CF_3SO_3)_3$·3H_2O in the crystal (120 K), showing the coordination geometry about the metal center and the hydrogen bonding network involving the anion and the unbound water molecules.

and the Ln−OH_2 distances do not follow this trend. The distance between the Ln^{3+} ion and the "capping" water molecule is therefore also proportionately longer for the smaller ions, reflecting the increase of nonbonding repulsive interactions between the ligand oxygen and the bound water molecule for the later lanthanide ions.

Structural Analysis of [$LnL^1(OH_2)$]$(CF_3SO_3)_3$·3H_2O]. Crystals of the lanthanide triflate complexes of the enantiopure tetra-amide ligand, L^1, were grown by slow evaporation from aqueous solution,[15] and included three water molecules of crystallization in the unit cell. The ligand in each case (Ln = Pr, Nd, Sm, Eu, Gd, Tb, Dy, Er, Yb, and Lu) adopted a regular square antiprismatic geometry, with an *R* configuration at the stereogenic center at carbon giving rise to a Λ configuration at the metal center and a *δδδδ* configuration for the C-4 related NCCN chelate rings involving the ring nitrogen.[13] In the case of Sm and Eu, the *SSSS* ligand was used, giving Δ−*λλλλ* complexes. The bound water molecule caps the square antiprism and acts as a hydrogen bond donor to two triflate counterions, and as a hydrogen bond acceptor to the nearest water molecule (Figure 4). Geometric parameters are given in Table 3. Plots of the variation of lanthanide/ligand-oxygen and Ln−OH_2 bond

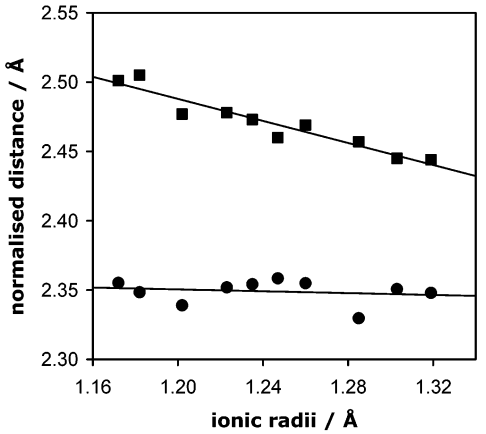

Figure 5. Variation of the Ln−OH_2 bond distances (upper) and the lanthanide−ligand O distances for the isomorphous and isostructural series [$LnL^1(OH_2)$]$(CF_3SO_3)_3$·3H_2O (Ln = Pr, Nd, Sm, Eu, Gd, Tb, Dy, Er, Yb, Lu) crystallizing in $P2_1$. Ln−O distances have been normalized (referenced to Gd) to account for the ionic radius variation.

Table 3. Summary of Geometric Parameters for [$LnL^1(OH_2)_2$]$(CF_3SO_3)_3$·3H_2O

		normalized distances/Å		absolute distances/Å	
M	*r*/Å[14]	M−O	M−$L_{(av)}$	M−O	M−$L_{(av)}$
Pr	1.319	2.450	2.341	2.516(3)	2.420
Nd	1.303	2.453	2.353	2.501(2)	2.407
Sm	1.285	2.456	2.330	2.495(4)	2.368
Eu	1.260	2.464	2.355	2.482(2)	2.368
Gd	1.247	2.466	2.360	2.460(2)	2.359
Tb	1.235	2.473	2.354	2.461(2)	2.342
Dy	1.223	2.478	2.349	2.454(2)	2.328
Er	1.202	2.477	2.339	2.432(2)	2.294
Yb	1.182	2.505	2.349	2.440(2)	2.284
Lu	1.172	2.501	2.355	2.426(2)	2.280

Scheme 1

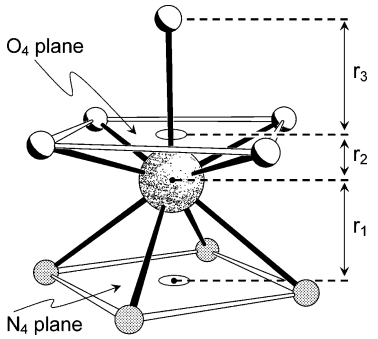

distances across the series reveal the same features as those observed for the $[Ln(OH_2)_9]^{3+}$ and [$LnDOTA(OH_2)$]$^-$ complexes. In this case, the normalized Ln−OH_2 distance is elongated by 0.05 Å (from Pr to Lu) while the ligand donor to lanthanide ion bond distances again simply echo the ionic radius variation (Figure 5).

A detailed analysis of variations in the coordination polyhedron across the series has been carried out.[16] Using the parameters defined in Scheme 1, significant variations were observed. The geometric parameters examined included the area defined by the N_4 rectangle, the area defined by the ligand O_4 rectangle, the distance of the metal ion above or below the N_4 and O_4 centroids r_1 and r_2, and the distance of the bound water oxygen to the centroid of the O_4 plane, r_3. The distance of the bound water molecule to the N_4 centroid

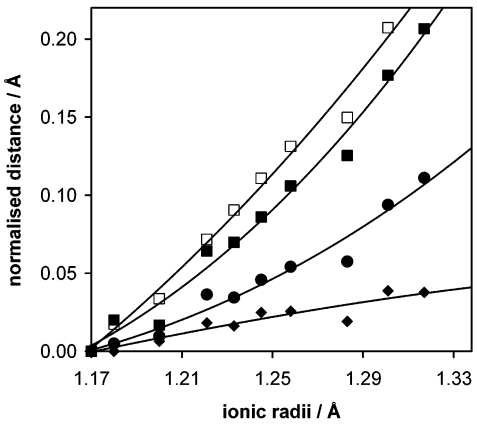

Figure 6. Variation of the change in the distances across the Ln series between the N_4 and O_4 planes (◆) in $[Ln{\cdot}L^1(OH_2)]^{3+}$, compared to the distances from the centroid of the N_4 plane to the metal ion (●) and to the bound water molecule (■). The change in the mean distance between the axial water oxygen and the ligand amide carbonyl oxygens is also shown (□).

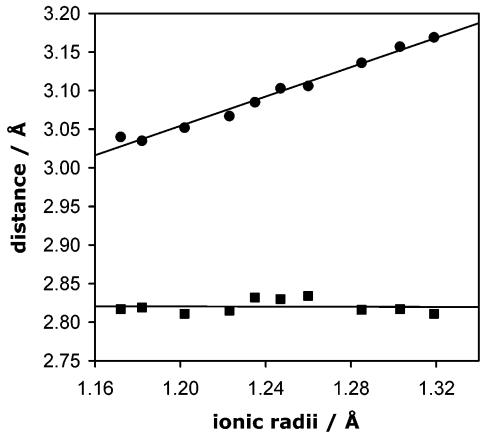

Figure 7. Variation of the distances between the coordinated water oxygen in $[LnL^1(OH_2)](CF_3SO_3)_3{\cdot}3H_2O$ (Ln = Pr, Nd, Sm, Eu, Gd, Tb, Dy, Er, Yb, Lu) and (i) the nearest triflate oxygen (■); (ii) the second sphere water oxygen (●).

is then given by ($r_1 + r_2 + r_3$), where $r_2 + r_3$ is the metal−water bond distance. In addition, the area defined by the four triangles, each involving an edge of the O plane and the metal ion, was measured. This provides a reasonable measure of the "approach area" for solvent access. This latter parameter decreased linearly from 10.3 Å^2 for the Lu complex to 11.6 Å^2 for the Pr analogue, consistent with an increase in solvent accessibility in the lighter lanthanide complexes.

Examination of the change in the areas of the quadrangles defined by the N_4 and O_4 atoms (each was essentially coplanar) revealed that the smaller N_4 area decreased only by 4% from Pr to Lu, whereas the O_4 area fell by 16%. Such variations are expected in view of the constrained rigidity of the 12-N_4 ring and indicate that the O_4 donor array (and the OLnO angles) expands significantly, as the Ln ion size increases. The "pinching in" of the O_4 plane, as the metal ion size reduces, is not accompanied by any change in the separation of the N_4 and O_4 planes. Further information on the relative position of the Ln ion is given by comparing the relative distance of the metal ion with respect to the N_4 and O_4 planes, in relation to the metal−water bond length. Thus, the distance between the N_4/O_4 planes ($r_1 + r_2$ in Scheme 1) changes relatively little, an elongation of 0.03 Å from Lu to Pr, while the distance from the N_4 basal plane to both the metal ion (r_1) and the water molecule ($r_1 + r_2 + r_3$) increases more significantly. Indeed, the latter distance increases by a factor of 2 more than the former, across the series (Figure 6), consistent with the positioning of the larger ions (Pr, Nd) relatively nearer to the O_4 plane. For the smaller ions, as the ion sits down more onto the N_4 plane, the water molecule is then brought closer to the O_4 donor atoms and is subject to increased nonbonded repulsion. This effect is borne out by analyzing the change in the mean distance between the coordinated water oxygen and the ligand oxygen donors, which falls from 2.966 Å for Pr to 2.732 Å for Lu.

In summary, the apical bound water molecule is in a sterically demanding position, and this effect is most apparent for the smaller lanthanide ions. This leads to a relative lengthening of the Ln−OH_2 bond (Figure 5), which can also be regarded as a weakening of the Ln−water electrostatic interaction from Pr to Lu, associated with destabilization of the ground state structure.

Discussion

The structural analysis of the Ln−OH_2 bond length variation for the nine-coordinate aqua ions, the anionic complex $[LnDOTA(H_2O)]^-$, and the cationic tetra-amide complex, $[Ln{\cdot}L^1(OH_2)]^{3+}$, reveals a common feature. The capping water molecule is in a sterically demanding position and is longer for the smaller ions than anticipated on the basis of ionic radii changes, as a result of increasing repulsive nonbonded interactions with adjacent donors. The change from La to Lu is estimated to be of the order of 0.05 (±0.01) Å in each case, after allowing for the ionic radius contraction (La 1.356 Å, Lu 1.172 Å).[14] A crude estimate of the change in the electrostatic binding energy (ΔH) associated with such an elongation can be calculated with the aid of density functional theory. The electrostatic binding energy (in vacuo) between an isolated water molecule and a point charge varies as r^{-1}. For an elongation of 0.06 Å between 2.44 and 2.50 Å, the electrostatic potential energy decreases by 2.4 kJ mol^{-1} per unit of charge of the Ln ion center. At the same time, the hydrogen bond acceptor ability of the bound water is significantly perturbed: the shorter the Ln−OH_2 bond, the less effective it should be as a hydrogen bond acceptor. Across the series (Pr to Lu), the distance between the bound water oxygen and the triflate oxygen (reflecting H-bond donor ability) in $[Ln{\cdot}L^1(OH_2)](CF_3SO_3)_3{\cdot}3H_2O$ remains invariant across the series (Figure 7) while the distance between the bound water oxygen and the second-sphere water oxygen (reflecting H-bond acceptor ability) changes from 3.169 (Pr) to 3.040 Å (Lu).

Such features are of particular interest in developing a better understanding of the transition state structure for water interchange. Inspection of space-filling models for $[Ln{\cdot}L^1(OH_2)]^{3+}$ reveals that a 10-coordinate structure is very sterically hindered, even for La, so that the water interchange process is likely to proceed via a predominantly dissociative process, at least for the central and later Ln ions, as suggested

in the reported studies of related lanthanide complexes giving positive values of $\Delta S^{\ddagger}$ and $\Delta V^{\ddagger}$, from the *T* and *P* dependence of the rate of water exchange.[13,17,18] Features which lead to a destabilization of the ground state structure or a stabilization of the putative transition state structure should lower the free energy of activation for dissociative water interchange. The structural studies described here allow assessment of the relative importance of ground state destabilization and will have the most significance in complexes where the transition state closely resembles the ground state structure. The lengthening of the Ln−water, accompanied by the shortening of the bound/second sphere water distance across the series, can be considered as an early snapshot of the developing transition state structure. For the cationic Eu and Yb triflate complexes of L^1, the water exchange rate (298 K) has been estimated to be 500 times faster for the Yb complex.[13] Such an enhancement (not as originally surmised due to a change in the coordination geometry, see ref 19) in rate of 2 orders of magnitude (from Eu to Yb) is also seen for the Eu/Yb complexes of DOTAM, L^3, and the glycinate ester analogue, L.[49,18] This equates to a difference in the free energy of activation of about 13 kJ mol^{-1} (298 K). Although it is tempting to relate part of this rate enhancement to the raising of the relative ground state energy of the Yb complex, it is likely that there is a very significant entropy term to consider, associated with the release of ordered water molecules in the second hydration sphere.

The earlier lanthanide complexes of L^1, L^3, and L^4 (Ce, Pr) also undergo faster water exchange than the Eu analogue, by factors of between 30 and 70. In this case, given that the $Ln-OH_2$ bond length is *relatively* shorter for the larger ions, it is likely that the transition state structure no longer resembles the ground state and its position is either "late" or the interchange mechanism may even be somewhat associative in character. This idea is consistent with the increase in the "approach area" for solvent access for the earlier Ln ions already defined, and it can in principle be tested by more detailed variable *T*/*P* rate studies.

Conclusion

In nine-coordinate lanthanide complexes adopting a common tricapped trigonal prismatic or monocapped square-antiprismatic structure, the capping ligand occupies a sterically demanding position. As the lanthanide series is traversed, the bond length of the capping water molecule becomes longer for the smaller ions, as a result of unfavorable intramolecular nonbonding interactions. This is the case for lanthanide complexes of DOTA, L^2, the chiral tetramide ligand, L^1, and the $[Ln(OH_2)_9]^{3+}$ ions themselves. Thus, for a dissociative water exchange process, the destabilization of the $Ln-OH_2$ bond, accompanied by an enhancement in its hydrogen bond acceptor ability, may partly explain the enhanced rate of water exchange observed for cationic complexes of the later Ln ions (e.g., Yb, Tm) compared to the central ions (Eu, Gd).

Acknowledgment. We thank EPSRC for support.

Supporting Information Available: Crystallographic data in CIF format. This material is available free of charge via the Internet at http://pubs.acs.org.

IC030203Z